CHEMISTRY
A European Journal

Accepted Article

Title: Alkali-phosphonate-MOFs

Authors: Gündoğ Yücesan, Maria Maares, M. Menaf Ayhan, Kai B. Yu, A. Ozgur Yazaydin, Kevser Harmandar, Hajo Haase, Jens Beckmann, and Yunus Zorlu

COMMUNICATION

Alkali-phosphonate-MOFs

Maria Maares[a], M. Menaf Ayhan[b], Kai. B. Yu[c], A. Ozgur Yazaydin[c], Kevser Harmandar[b], Hajo Haase[a], Jens Beckmann[d], Yunus Zorlu* [b], and Gündoğ Yücesan*[a]

Abstract: We report a new family of porous MOFs namely alkali-phosphonate-MOFs. [Na$_2$Cu(H$_4$TPPA)]·(NH$_2$(CH$_3$)$_2$)$_2$ (**GTUB-1**) was synthesized using the tetratopic 5,10,15,20-Tetrakis[p-phenylphosphonic acid] porphyrin (**H$_8$-TPPA**) linker with planar X-shaped geometrical core. **GTUB-1** is composed of rectangular void channels with BET surface area of 697 m^2/g. GTUB-1 exhibits exceptional thermal stability. The toxicity analysis of the (**H$_8$-TPPA**) linker indicates that it is well tolerated by an intestinal cell line, suggesting its suitability for creating phosphonate-MOFs for biological applications.

Metal organic frameworks (MOFs) are a recently emerging family of microporous materials. [1] MOFs combine organic and inorganic functions on the same platform to create rationally designed pore sizes [1-4], and they provide a wide range of application areas based on the host-guest interactions in their pore sites. Some of the MOF applications includes small molecule storage, catalysis, fuel cell applications, drug delivery etc. [2, 5-9] In addition, the possibility of post-synthetic modifications makes MOFs technologically more advanced compared to the traditional microporous materials such as Zeolites. [10, 11] To date, there are more than 50.000 MOF crystal structures that have been reported in the literature, and the corresponding CIF files are deposited into the crystal structure databases. [12] Identity of organic linkers and inorganic building units (IBUs) determine the characteristics of the synthesized MOFs. One goal yet to be achieved in MOF chemistry is to create pathways to synthesize them with alkali-IBUs. [13-14] The systematic introduction of alkali-IBUs into MOF synthesis would be important especially with respect to the biological applications of MOFs in the future or creating edible-MOFs for drug delivery purposes. To date, there are limited examples of porous MOFs that are constructed with alkali metals. Two of the most prominent examples include Yaghi's work with L-Aspartate bridging linkers and Stoddart's work where they used commercially available cyclodextrins (CD) to form CD-MOFs using a set of alkali metals. [13-15] These findings were groundbreaking as they were the first examples of edible MOFs synthesized using commercially available edible resources. Alkali CD-MOFs have been proven to be efficient drug delivery agents where the ibuprofen encapsulated MOFs improved the half-life and the solubility of the ibuprofen molecule. [15] The next step would be designing novel non-toxic linker architectures encompassing a variety of metal binding functional groups to create novel MOFs for pharmaceutical and food chemistry applications.

Phosphonate-MOFs are recently emerging as the novel and extremely stable family of MOFs. [16] Phosphonates have relatively higher affinity for alkali metal ions compared to the conventional carboxylate-MOFs. [17, 18] In addition, there are several biochemical pathways that are dependent on the presence of phosphonate functional group. [19] For example, our previously reported zinc-organophosphonate cage structure was readily tolerated by intestinal cell lines indicating their potential significance for biological applications. [20] Notably, alkali-phosphonate-MOFs possess great potential for biological applications, to the best of our knowledge, there is no porous phosphonate-MOFs reported with alkali-IBUs in the literature yet and alkali-MOFs are quite rare. [13-15] The presence of alkali metals in dense organodiphosphonate metal organic solids is a clear indication that alkali metals could also create porous networks with appropriate linker geometries. [21] Therefore, we have decided to explore the potential of tetratopic planar phosphonate linker **H$_8$-TPPA** (See Fig. 1) in forming alkali-phosphonate-MOFs and we report the first-time synthesis of a porous alkali-phosphonate-MOF namely **GTUB-1** using the **H$_8$-TPPA** linker with planar X-shaped core geometry. We have also studied the crystal structure of the **GTUB-1**, its surface area, and the toxicity studies of the **H$_8$-TPPA linker.**

H$_8$-TPPA was synthesized via two different synthetic methods as seen in Scheme S1. The reaction of **H$_8$-TPPA** with Cu(NO$_3$)$_2$.3H$_2$O in DMF/MeOH and NaOH at 120 °C yielded red plate-shaped single crystals of **GTUB-1**. The structure of GTUB-1 was obtained using single crystal x-ray diffraction (see SI for crystallographic details). The crystal structure of GTUB-1 is composed of a novel one-dimensional Na-O-P inorganic building unit (Fig. 1b), which is connected by **H$_8$-TPPA** moieties (Fig. 2a) to form the rectangular void channels (Fig. 2c). The inorganic building unit is new and unique to **GTUB-1**. The 1D alkali-phosphonate-IBU is composed of Na-O rhombus chain where these rhombi are connected by Na-O-Na and O-P-O bridges to create the 1D alkali-IBU (Fig. 2b). Previously reported Na-MOFs by Yaghi are composed of 2D alkali-IBUs and linear L-aspartate, which created surface areas of 216 and 231 m^2/g. [13] As it is expected, the use of the tetraphosphonic acid based metalloporphyrin (**H$_8$-TPPA**) with 2 nm long linker length (Fig. 2a) helped create dramatically larger surface area of 697 m^2/g

[a]   Lebensmittelchemie und Toxikologie, Technische Universität Berlin, Berlin, Gustav-Meyer-Allee-25, 13355, Germany
        E-mail: yuecesan@tu-berlin.de
[b]   Department of Chemistry, Gebze Technical University, Gebze, 41400, Kocaeli, Turkey
        E-mail: yzorlu@gtu.edu.tr
[c]   Department of Chemical Engineering, University College London, London WC1E 7JE, UK
[d]   Institut für Anorganische Chemie und Kristallographie, Universität Bremen, Leobener Straße, 28359 Bremen, Germany

        Supporting information for this article is given via a link at the end of the document.
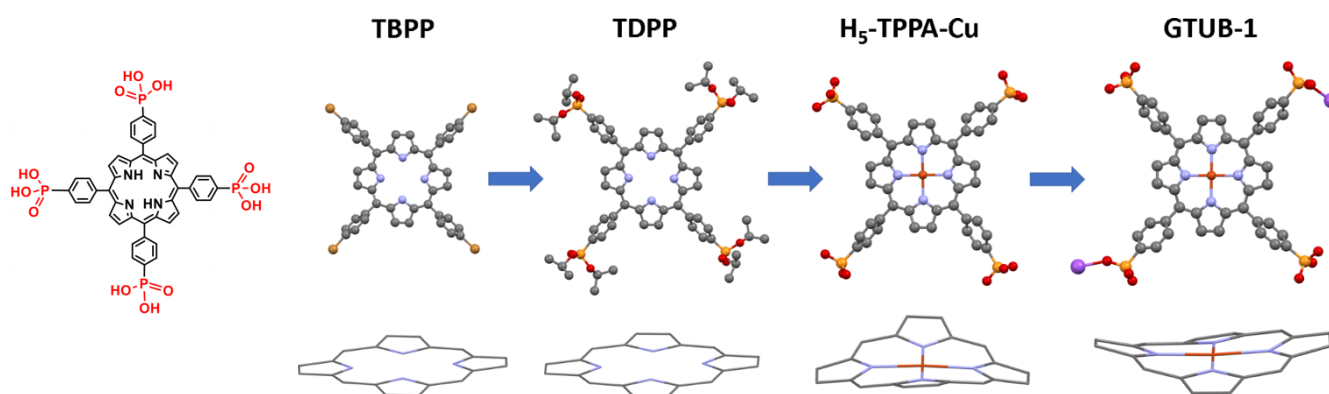
COMMUNICATION

Figure 1. Evolution of alkali-phosphonate-MOFs from simple precursors; the crystal structures of 5,10,15,20-tetrakis(4-bromophenyl)porphyrin (TBPP), 5,10,15,20-Tetrakis[p-(diisopropoxyphosphoryl)phenyl] porphyrin (TDPP), copper complex of 5,10,15,20-Tetrakis [p-phenylphosphonic acid] porphyrin (H$_4$-TPPA-Cu), and GTUB-1 showing planar and non-planar (saddle) deformations of the porphyrin macrocycles. The meso-aryl substituents and hydrogen atoms were omitted to better illustrate the conformations of the porphyrin macrocycles.

compared to the previous Na-MOFs (See SI for experimental details). [13] The structure of **GTUB-1** is similar to the previously reported phosphonate-MOFs, which are composed of 1D-IBUs and tetratopic phosphonate linkers. [24, 27-30] The 90° of angle between the phosphonate tethers of **H$_8$-TPPA** linker was influential in creating the rectangular voids (Fig. 1c). Bulky porphyrin core of **H$_8$-TPPA** produced lower surface areas compared to the tetrahedral phosphonate-MOFs with 1D IBUs. But 698 m^2/g surface area of **GTUB-1** is very close to the 700 m^2/g surface area of recently reported [Co$_2$(Ni-H$_4$TPPA)]·2 DABCO·6 H$_2$O. [29] Cu(II) ions preferred to occupy the center of the porphyrin ring.

Martell's early work from 70s and later Demadis indicated that phosphonates have relatively higher affinity towards the alkali metals compared to the other metal binding functional groups, such as carboxylates, and pyridines. [17, 22] Usually, it is very difficult to crystallize phosphonate-MOFs as phosphonates undergo a fast reaction with transition metal ions creating immediate amorphous precipitates. [22, 23] Therefore, hydrothermal reaction conditions at high temperature, pressure and sometimes the presence of HF as a mineralizer are required to obtain metalphosphonate crystals. [23] Alkali metals have relatively lower affinities towards phosphonates compared to the transition metals. Therefore, it was possible to obtain the alkali-phosphonate-MOFs with aromatic tetratopic tetraphosphonate linker **H$_8$-TPPA** (Scheme S1, see ESI) using the conventional MOF crystallization methods in this study. [1-4] One dimensional IBUs in phosphonate metal organic solids usually produce dense lamellar or pillared layered frameworks. [16] In order to avoid the formation of regularly observed dense-lamellar and pillared-layered metal organic solids we used a tetraphosphonic acid having a planar porphyrin core [16]. The crystal structure of **GTUB-1** indicates that the overlaid **H$_8$-TPPA** linkers in **GTUB-1** are piled linearly with 3.786 and 4.048 Å (Fig. 2e). This orientation of the **H$_8$-TPPA** linker in **GTUB-1** is very similar to the π-stacking orientation of the aryl linkers in the previously reported dense lamellar and pillared layered phosphonate metal organic solids. [16] The unique X-shaped planar geometry and 90° angular separation between the phenylphosphonate tethers of **H$_8$-TPPA** linker were influential in creating the nanosized rectangular channels along the a-axis with the dimensions of 9.78 x7.73 Å in

GTUB-1. The crystal structure of the phosphonatediester form of free **TDPP** linker is distinct from **GTUB-1**'s porphyrin orientation, as non-polar isopropyl groups at the end of phenyl tethers could approach to the non-polar space between the phenyl tethers of porphyrin core (See Fig. 1). Therefore, the presence of polar 1D alkali-phosphonate-IBU is the driving force in forming the void spaces in **GTUB-1**.
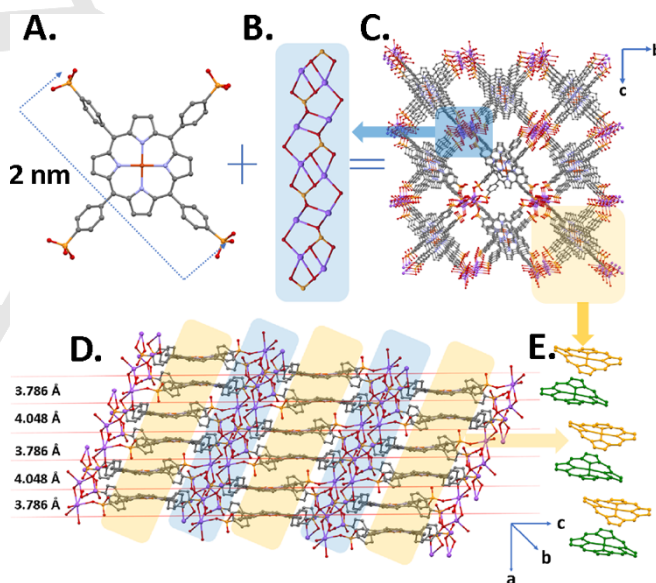

Figure 2. (**A**). Representation of the porphyrin building block based on H$_4$-TPPA-Cu (**B**) View of one-dimensional Na-O-P inorganic building unit (IBU) (**C**). The perspective view of the rectangular void channels viewed down a-axis (**D**) and (**E**). The assembly of the slipped-stack structure (offset stacking) of porphyrine macrocycles.

As future research aims to use alkali-phosphonate-MOFs for biological implementations, applying it as a delivery tool for drugs or micronutrients via the intestinal epithelium, its toxicity on intestinal cells was investigated. To this end, cell viability of the intestinal cell line Caco-2 after long-term incubation (24 h) with different amounts of **H$_8$-TPPA** was investigated by analyzing mitochondrial enzyme activity of the cells (Fig. 3). Treatment of

WILEY-VCH

COMMUNICATION

Caco-2 cells with this compound caused no cytotoxicity, even at high concentrations. Comparable to the previously reported zinc-organophosphonate cage [20]. **H₈-TPPA** is not toxic for intestinal cells at the investigated concentrations, making it suitable for further cellular applications *in vitro* and *in vivo*.
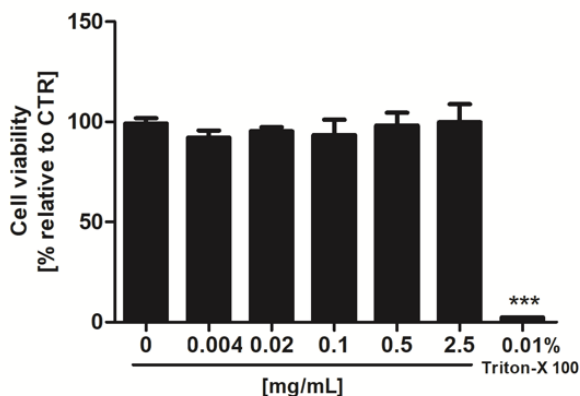
Figure 4. Thermogravimetric analysis of **TDPP**, **H₈-TPPA** and **GTUB-1**

Figure 3. Cytotoxicity of H₈-TPPA on intestinal cells: Shown is the cell viability of differentiated Caco-2 cells after treatment with different concentrations of **H₈-TPPA** (0-2.5 mg/ml) for 24 h. Cell viability was analyzed by measuring mitochondrial enzyme activity using a tetrazolium salt solution and is displayed as percent of solvent control (cell culture media with 2.5 % DMSO). A total of 0.01 % triton X-100 was used as positive control for cytotoxicity. Data are shown as means + standard deviation of three independent experiments and significant differences are indicated (***p < 0.001; One-way ANOVA with Dunnett's multiple comparison test).

As seen in Fig. 4, the TGA analysis of **TDPP** and **H₈TPPA** indicate that the diester form TDPP starts to decompose at ca. 250 ºC and **H₈TPPA** starts to decompose at ca. 300 ºC. The relative high stability of the linker with porphyrin core is clear indication that this family of alkali-phosphonate-MOFs could create thermally stable MOFs and the sodium coordination on the **H₈TPPA** linker makes the thermal stability more interesting as the linker components of **GTUB-1** now starts to decompose at ca. 400 ºC where the total decomposition of organic components ends at ca. 525 ºC. The thermal behavior is much better compared to Yaghi's Na-MOFs with L-aspartate linkers, which started to decompose at ca. 350 ºC and totally decomposed at ca. 450 ºC. [13] Alkali cyclodextrin MOFs start to decompose between 175 and 200 ºC. [14] To the best of our knowledge **GTUB-1** is the most thermally stable porous alkali-MOF reported in the literature.
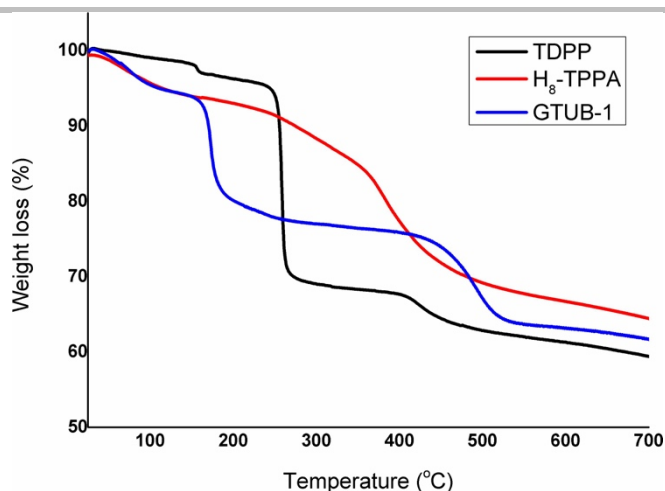
In conclusion, we report **GTUB-1** as the first member of a new family of MOFs namely porous alkali-phosphonate-MOFs in the literature. **GTUB-1** has substantially larger surface area of 697 m²/g compared to the previously reported Na-MOFs. [13] The relatively high affinity of phosphonate units towards alkali metal ions has favored the crystallization of phosphonate-MOFs under mild and conventional MOF crystallization methods eliminating the need for hydrothermal reactions. **H₈-TPPA** linker is well tolerated by intestinal Caco-2 cell lines. Toxicity pattern of the **H₈-TPPA** linker can be further studied to produce biocompatible or edible MOFs using biologically significant metal ions. The superior thermal decomposition pattern of **GTUB-1** is clear indication of its potential for industrial applications.

[1]   O. M. Yaghi, M. O'Keeffe, N. W. Ockwig, H. K. Chae, M. Eddaoudi, J. Kim, *Nature* **2003**, 423, 705-714.

[2]   H. Furukawa, K. E. Cordova, M. O'Keeffe, O. M. Yaghi, *Science* **2013,** 341(6149), 1230444.

[3]   M. J. Kalmutzki, N. Hanikel, O. M. Yaghi, *Science Advances*, 2018, 4, 1-16.

[4]   A. Schoedel, M. Li, D. Li, M. O'Keeffe, O. M. Yaghi, *Chem. Rev.* **2016**, 116, 12466-12535.

[5]   M. Ranocchiari, J. A. van Bokhoven, *Physical Chem. Chem. Physics,* **2011**, 13, 6388-6396.

[6]   P. Horcajada, R. Gref, T. Baati, P.K. Allan, G. Maurin, P. Couvreur, G. Ferey, R.E. Morris, C. Serre, *Chem. Rev.* **2011**, 112, 1232–1268.

[7]   S. Rojas, T. Baati, L. Njim, L. Manchego, F. Neffati, N. Abdeljelil, S. Saguem, C. Serre, M. F. Najjar, A. Zakhama, P. Horcajada, *J. Am. Chem. Soc.* **2018**, 140, 9581-9586.

[8]   G. M. Espallargas, E. Coronado, *Chem. Soc. Rev.* **2013**, 42, 1525-1539.

[9]   G. M. Espallargas, E. Coronado, *Chem. Soc. Rev.* **2018**, 47, 533-557.

[10]   M. S. Cohen, *J. Am. Chem. Soc.* **2017**, 139, 2855-2863.

WILEY-VCH

COMMUNICATION

[11]   Z. Wang, S. M. Cohen, *Chem. Soc. Rev.,* **2009**, 38, 1315-1329.

[12]   P. Z. Moghadam, A. Li, S. B. Wiggin, A. Tao, A. G. P. Maloney, P. A. Wood, S. C. Ward, D. Fairen-Jimenez*, Chem. Mater.* **2017**, 29 , 2618 - 2625.

[13]   P. Simon, C. A. Trickett, H. Furukawa, O. Yaghi, *ChemComm.* **2015**, 51, 17463-17466.

[14]   R. A. Smaldone, R. S. Forgan, H. Furukawa, J. J. Gassensmith, A. M. Z. Slawin, O. M. Yaghi, J. F. Stoddart, *Angew. Chem. Int. Ed.* 2010, 49, 8630-8634.

[15]   K. J. Hartlieb, D. P. Ferris, J. M. Holcroft, I. Kandela, C. L. Stern, M. S. Nassar, Y.Y. Botros, J. Fraser Stoddart, *Mol. Pharmaceutics* **2017**, 14, 1831-1839.

[16]   G. Yücesan, Y. Zorlu, M. Stricker, J. Beckmann, *Coord. Chem. Rev.* **2018**, 369, 105-122.

[17]   R. Motekaitis, I. Murase, A. E. Martell, *Inorg. Chem*. 1976, 15, 2303.

[18]   T. K. Hurst, D. Wang, R. B. Thompson, C. A. Fierke, *Biochim. Biophys. Acta* **2010**, 1804, 393-403.

[19]   D. A. Born, E. C. Ulrich, K. S. Ju, S. C. Peck, W. A. van der Donk, C. L. Drennan, *Science*, **2017**, 358, 1336-1338.

[20]   A. Bulut, M. Maares, K. Atak, Y. Zorlu, B. Çoşut, J. Zubieta, J. Beckmann, H. Haase, G. Yücesan, *CrystEngComm*, **2018**, 20, 2152-2158.

[21]   G. Yücesan, V. Golub, C. J.O'Connor, J. Zubieta, *Inorg. Chim. Acta*, **2006**, 359, 1637-1642.

[22]   I. R. Salcedo, R. M. P. Colodrero, M. Bazaga-García, A. Vasileiou, M. Papadaki, P. Olivera-Pastor, A. Infantes-Molina, E. R. Losilla, G. Mezei, A. Cabeza, K. D. Demadis, *CrystEngComm*. **2018**, 20, 7648-7658.

[23]   K. J. Gagnon, H. P. Perry, A. Clearfield, *Chem. Rev.*, **2012**, 112, 1034-1054.

[24]   A. Schütrumpf, A. Bulut, N. Hermer, Y. Zorlu, E. Kirpi, N. Stock, A. O. Yazaydin, G. Yücesan, J. Beckmann, *ChemistrySelect*, **2017**, 2, 3035-3038.

[25]   A. Bulut, Y. Zorlu, E. Kirpi, A. Cetinkaya, M. Worle, J. Beckmann, G. Yücesan, *Cryst. Growth Des.*, **2015**, 15, 5665-5669.

[26]   A. Schütrumpf, A. Duthie, E. Lork, G. Yücesan and J. Beckmann, *Z. Anorg. Allg. Chem.* **2018**, 644, 1134-1142.

[27]   Y. Zorlu, D. Erbahar, A. Çetinkaya, A. Bulut, T. S. Erkal, Ö. Yazaydın, J. Beckmann, G. Yücesan, *Chem.Commun.* **2019**, 55, 3053-3056.

[28]   T. Rhauderwiek, K. Wolkersdorfer, S. Oien-Odegaard, K. P. Lillerud, M. Wark, N. Stock, *Chem. Commun.* **2018**, 54, 389-392.

[29]   B. Wang, T. Rhauderwiek, A. K. Inge, H. Xu, T. Yang, Z. Huang, N. Stock, X. Zou, *Chem. Eur. J.*, **2018**, 27, 17429-17433.

[30]   T. Rhauderwiek, H. S. Zhao, P. Hirschle, M. Doblinger, B. Bueken, H. Reinsch, D. De Vos, S. Wuttke, U. Kolb and N. Stock, *Chem. Sci.*, **2018**, 9, 5467-5478.
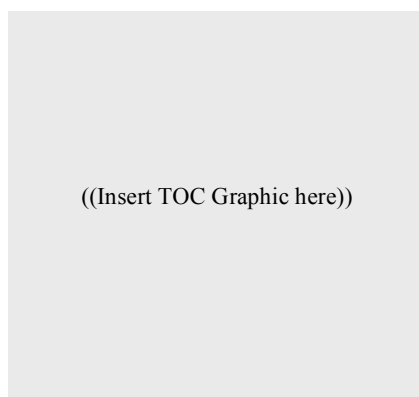
WILEY-VCH

COMMUNICATION

Entry for the Table of Contents (Please choose one layout)

Layout 1:

COMMUNICATION

Text for Table of Contents		*Author(s), Corresponding Author(s)**
		Page No. – Page No.
		Title
	((Insert TOC Graphic here))	

Layout 2:

COMMUNICATION

	Author(s), Corresponding Author(s)*
((Insert TOC Graphic here))	***Page No. – Page No.***
	Title

Text for Table of Contents